

# Diagnostic Performance of $^{18}\text{F}$ -FET PET in Newly Diagnosed Cerebral Lesions Suggestive of Glioma

Marion Rapp<sup>\*1</sup>, Alexander Heinzel<sup>\*2</sup>, Norbert Galldiks<sup>\*3,4</sup>, Gabriele Stoffels<sup>3</sup>, Jörg Felsberg<sup>5</sup>, Christian Ewelt<sup>6</sup>, Michael Sabel<sup>1</sup>, Hans J. Steiger<sup>1</sup>, Guido Reifenberger<sup>5</sup>, Thomas Beez<sup>1</sup>, Heinz H. Coenen<sup>3</sup>, Frank W. Floeth<sup>\*1,7</sup>, and Karl-Josef Langen<sup>\*3</sup>

<sup>1</sup>Department of Neurosurgery, Heinrich-Heine University, Düsseldorf, Germany; <sup>2</sup>Department of Nuclear Medicine, University Clinic Aachen, Aachen, Germany; <sup>3</sup>Institute of Neuroscience and Medicine, Forschungszentrum Jülich, Jülich, Germany; <sup>4</sup>Department of Neurology, University of Cologne, Cologne, Germany; <sup>5</sup>Institute of Neuropathology, Heinrich-Heine University, Düsseldorf, Germany; <sup>6</sup>Department of Neurosurgery, University of Münster, Münster, Germany; and <sup>7</sup>Department of Spine and Pain, St. Vinzenz Hospital, Düsseldorf, Germany

The aim of this study was to assess the clinical value of O-(2- $^{18}\text{F}$ -fluoroethyl)-L-tyrosine ( $^{18}\text{F}$ -FET) PET in the initial diagnosis of cerebral lesions suggestive of glioma. **Methods:** In a retrospective study, we analyzed the clinical, radiologic, and neuropathologic data of 174 patients (77 women and 97 men; mean age,  $45 \pm 15$  y) who had been referred for neurosurgical assessment of unclear brain lesions and had undergone  $^{18}\text{F}$ -FET PET. Initial histology ( $n = 168$ , confirmed after surgery or biopsy) and the clinical course and follow-up MR imaging in 2 patients revealed 66 high-grade gliomas (HGG), 77 low-grade gliomas (LGG), 2 lymphomas, and 25 nonneoplastic lesions (NNL). In a further 4 patients, initial histology was unspecific, but during the course of the disease all patients developed an HGG. The diagnostic value of maximum and mean tumor-to-brain ratios ( $\text{TBR}_{\text{max}}/\text{TBR}_{\text{mean}}$ ) of  $^{18}\text{F}$ -FET uptake was assessed using receiver-operating-characteristic (ROC) curve analyses to differentiate between neoplastic lesions and NNL, between HGG and LGG, and between high-grade tumor (HGG or lymphoma) and LGG or NNL. **Results:** Neoplastic lesions showed significantly higher  $^{18}\text{F}$ -FET uptake than NNL ( $\text{TBR}_{\text{max}}$ ,  $3.0 \pm 1.3$  vs.  $1.8 \pm 0.5$ ;  $P < 0.001$ ). ROC analysis yielded an optimal cutoff of 2.5 for  $\text{TBR}_{\text{max}}$  to differentiate between neoplastic lesions and NNLs (sensitivity, 57%; specificity, 92%; accuracy, 62%; area under the curve [AUC], 0.76; 95% confidence interval [CI], 0.68–0.84). The positive predictive value (PPV) was 98%, and the negative predictive value (NPV) was 27%. ROC analysis for differentiation between HGG and LGG ( $\text{TBR}_{\text{max}}$ ,  $3.6 \pm 1.4$  vs.  $2.4 \pm 1.0$ ;  $P < 0.001$ ) yielded an optimal cutoff of 2.5 for  $\text{TBR}_{\text{max}}$  (sensitivity, 80%; specificity, 65%; accuracy, 72%; AUC, 0.77; PPV, 66%; NPV, 79%; 95% CI, 0.68–0.84). Best differentiation between high-grade tumors (HGG or lymphoma) and both NNL and LGG was achieved with a  $\text{TBR}_{\text{max}}$  cutoff of 2.5 (sensitivity, 79%; specificity, 72%; accuracy, 75%; AUC, 0.79; PPV, 65%; NPV, 84%; 95% CI, 0.71–0.86). The results for  $\text{TBR}_{\text{mean}}$  were similar with a cutoff of 1.9. **Conclusion:**

$^{18}\text{F}$ -FET uptake ratios provide valuable additional information for the differentiation of cerebral lesions and the grading of gliomas.  $\text{TBR}_{\text{max}}$  of  $^{18}\text{F}$ -FET uptake beyond the threshold of 2.5 has a high PPV for detection of a neoplastic lesion and supports the necessity of an invasive procedure, for example, biopsy or surgical resection. Low  $^{18}\text{F}$ -FET uptake ( $\text{TBR}_{\text{max}} < 2.5$ ) excludes a high-grade tumor with high probability.

**Key Words:** O-(2- $^{18}\text{F}$ -fluoroethyl)-L-tyrosine;  $^{18}\text{F}$ -FET PET; cerebral lesions; tumor

**J Nucl Med 2013; 54:229–235**

DOI: 10.2967/jnumed.112.109603

Conventional contrast-enhanced MR imaging is the diagnostic method of choice for primary brain tumors, but the specificity of conventional MR imaging for differentiating neoplastic lesions from nonspecific changes in brain tissue is limited (1). In combination with MR imaging, PET using radiolabeled amino acids is a valuable method to improve diagnostic accuracy for cerebral glioma. Of particular concern are the need for improved delineation of solid tumor tissue for biopsy guidance and treatment planning (2), treatment monitoring (3), and detection of brain tumor recurrence (4).

The most widely used tracer for amino acid PET is L-methyl- $^{11}\text{C}$ -methionine ( $^{11}\text{C}$ -MET), but its use is limited to PET centers with a cyclotron because of its short physical half-life (20 min) (5). O-(2- $^{18}\text{F}$ -fluoroethyl)-L-tyrosine ( $^{18}\text{F}$ -FET) is a well-established  $^{18}\text{F}$ -labeled amino acid for PET (half-life, 110 min) that shows logistic advantages over  $^{11}\text{C}$ -MET for clinical practice (6,7). Clinical results in brain tumors with PET have been reported to be similar between  $^{11}\text{C}$ -MET and  $^{18}\text{F}$ -FET (8).

The role of amino acid PET in the differential diagnosis of primary brain tumors is still being debated. In the largest study to date evaluating  $^{11}\text{C}$ -MET PET in a consecutive series of 196 patients with suspected brain tumors, differentiation between gliomas and nonneoplastic lesions (NNL) was achieved with a sensitivity of 76% and a specificity of

Received Jun. 2, 2012; revision accepted Sep. 17, 2012.

For correspondence or reprints contact: Karl-Josef Langen, Institute of Neuroscience and Medicine, Forschungszentrum Jülich, Wilhelm-Johnen Strasse, D-52425 Jülich, Germany.

E-mail: k.j.langen@fz-juelich.de

\*Contributed equally to this work.

Published online Dec. 11, 2012

COPYRIGHT © 2013 by the Society of Nuclear Medicine and Molecular Imaging, Inc.

87% using a threshold of 1.47 for the mean tumor-to-brain ratio, resulting in 79% correct classifications (9). Because of limited availability and logistic disadvantages, PET using the short-lived  $^{11}\text{C}$ -MET is increasingly being replaced by PET using  $^{18}\text{F}$ -labeled amino acids.

Only a few studies with limited patient populations have addressed the role of  $^{18}\text{F}$ -FET PET in the differential diagnosis of primary brain tumors. In the currently largest series of 88 patients with primary brain tumors,  $^{18}\text{F}$ -FET PET yielded a sensitivity of 93% for detecting a malignant tumor entity, and the negative predictive value (NPV) for a malignant entity was 89% (10). These results, however, were based only on a visual rating, and histology was available in only two thirds of patients. A recent metaanalysis of  $^{18}\text{F}$ -FET PET in 401 patients yielded a pooled sensitivity of 82% and a specificity of 76% for the diagnosis of a primary brain tumor (11). That analysis, however, was limited by variations in ROI definitions and acquisition times among the different studies.

The aim of this retrospective study was to further explore the diagnostic performance of  $^{18}\text{F}$ -FET PET in a large series of 174 strictly selected patients with suspected cerebral glioma on MR imaging and subsequent histologic confirmation.

With regard to the possible role of  $^{18}\text{F}$ -FET PET in the clinical decision-making process, this study focused on the value of the method for differentiating between neoplastic lesions and NNLs and between high-grade gliomas (HGGs) and low-grade gliomas (LGGs). Furthermore, the value of  $^{18}\text{F}$ -FET PET for differentiating a high-grade tumor (i.e., HGG or lymphoma) on the one hand from an LGG or benign lesion on the other hand was considered.

## MATERIALS AND METHODS

### Patients

In a retrospective analysis, we identified 262 patients who were referred to the Department of Neurosurgery of the University of Düsseldorf between 2001 and 2010 for assessment of an intracerebral mass or lesions and underwent  $^{18}\text{F}$ -FET PET. From this database, subjects were selected who had newly diagnosed and completely untreated lesions that were suggestive of a cerebral glioma on contrast-enhanced MR imaging according to the neuro-radiologic report and who had undergone  $^{18}\text{F}$ -FET PET before any therapeutic interventions that might have influenced  $^{18}\text{F}$ -FET uptake in the tissue (surgery, biopsy, chemo- or radiotherapy, or radiosurgery). Furthermore, a definite neuropathologic diagnosis after stereotactic biopsy or open resection within 6 wk after MR and PET imaging had to be available. The Heinrich Heine University Ethics Committee approved the study. All subjects gave written informed consent for investigation by  $^{18}\text{F}$ -FET PET. A group of 172 patients met these inclusion criteria. Furthermore, we decided to include 2 additional patients without histologic evaluation for whom both the clinical course (response to treatment) and declining MR imaging findings clearly confirmed a benign lesion (1 intracerebral abscess and 1 unspecific lesion). Forty-nine patients were excluded because they had a recurrent tumor, 11 patients were excluded because the biopsy had been performed before the PET scan, and 30 patients had no histologic confirmation within 6 wk after  $^{18}\text{F}$ -FET PET.

Thus, the final group, which was included in the statistical evaluation, consisted of 174 patients (97 men and 77 women; mean age, 45 y; range, 2–84 y). Histology after surgery or biopsy revealed 66 HGGs, 77 LGGs, 2 intracerebral malignant B-cell lymphomas, and 25 NNLs. Four lesions were classified as occult glioma because histologic investigation of biopsies at initial diagnosis were nondiagnostic but  $^{18}\text{F}$ -FET PET was positive and all 4 patients developed an HGG in the further course of disease.

Clinical and demographic patient data (age, sex, and initial leading symptom of the lesion), MR imaging findings (lesion size, location, and contrast enhancement), results of  $^{18}\text{F}$ -FET PET (tumor-to-brain ratios), and neuropathologic diagnoses are summarized in Tables 1 and 2. Further details on each individual patient are given in Supplemental Table 1 (supplemental materials are available online only at <http://jnm.snmjournals.org>).

### $^{18}\text{F}$ -FET PET Imaging and Data Analysis

The amino acid *O*-(2- $^{18}\text{F}$ -fluorethyl)-L-tyrosine ( $^{18}\text{F}$ -FET) was produced via nucleophilic  $^{18}\text{F}$ -fluorination with a specific radio-activity of more than 200 GBq/ $\mu\text{mol}$  as described previously (12). All patients fasted for at least 12 h before the PET studies.

PET studies were acquired after intravenous injection of 200 MBq of  $^{18}\text{F}$ -FET using an ECAT EXACT HR+ scanner (Siemens Medical Systems, Inc.) in 3-dimensional mode (32 rings; axial field of view, 15.5 cm). For attenuation correction, transmission was measured with three  $^{68}\text{Ge}/^{68}\text{Ga}$  rotating line sources. After Fourier rebinning and correction for attenuation, random coincidences, scattered coincidences, and decay, 63 image planes were iteratively reconstructed (ordered-subsets expectation maximization, 6 iterations, 16 subsets) using the ECAT 7.2 software. The reconstructed image resolution was approximately 5.5 mm. In recent years (2006–2010) dynamic PET studies have been routinely acquired (0–50 min), but for earlier investigations (2001–2005) only static scans were available (15–40 min). The further evaluation was based on the summed PET data from 20 to 40 min after injection.

$^{18}\text{F}$ -FET PET and contrast-enhanced MR images were coregistered using MPI tool software (version 6.48; ATV). The transaxial slices showing the highest  $^{18}\text{F}$ -FET accumulation in the tumors were chosen for ROI analyses.  $^{18}\text{F}$ -FET uptake in the unaffected brain tissue was determined by a larger ROI placed on the contralateral hemisphere in an area of normal-appearing brain tissue including white and gray matter.  $^{18}\text{F}$ -FET uptake in the tumor was determined by a 2-dimensional autocontouring process using a tumor-to-brain ratio (TBR) of at least 1.6. This cutoff was based on a biopsy-controlled study in cerebral gliomas in that a lesion-to-brain ratio of 1.6 best separated tumoral from peritumoral tissue (2). When  $^{18}\text{F}$ -FET uptake in the lesions was similar to that in the normal brain tissue, a representative irregular ROI was placed manually on the area of signal abnormality in the T1- and T2-weighted transversal MR scan and transferred to the coregistered  $^{18}\text{F}$ -FET PET scan in each case. Mean and maximum TBR ( $\text{TBR}_{\text{mean}}$  and  $\text{TBR}_{\text{max}}$ ) were calculated by dividing the mean and maximum SUV of the tumor ROI by the mean SUV of normal brain in the  $^{18}\text{F}$ -FET PET scan.

### MR Imaging and Analysis

All patients had routine MR imaging using a 1.5-T MR scanner with a standard head coil before and after administration of gadolinium-diethylenetriaminepentaacetic acid (T1-, T2-, and fluid-attenuated inversion recovery sequences; slice thickness of 4–6 mm). The MR imaging was performed within 6 wk before

**TABLE 1**  
Patient Characteristics

Diagnosis	Patients (n)	Mean age (y)	Sex (n)		Initial leading symptom (n)			
			Male	Female	Increased ICP	Neurologic deficit	Seizure	Asymptomatic, unspecific, or incidental
All	174	45	97	77	29	25	89	31
NNLs	25	48	18	7	2	8	6	9
Hematoma	4	57	4	0	2	1	1	—
Demyelinating lesion	5	40	3	2	—	4	—	1
Abscess	6	49	6	0	—	2	1	3
Unspecific histology	10	47	5	5	—	1	4	5
Neoplastic lesions	149	44	79	70	27	17	83	22
Occult glioma	4	46	0	4	—	—	4	—
Glioma WHO I	4	43	2	2	3	1	—	—
Diffuse glioma WHO II	73	41	38	35	13	8	44	8
Astrocytoma II	53	42	28	25	9	4	33	7
Oligoastrocytoma II	12	39	7	5	3	2	6	1
Oligodendroglioma II	6	41	3	3	—	2	4	—
Ependymoma II	2	23	0	2	1	—	1	—
Anaplastic glioma WHO III	47	42	25	22	6	5	27	9
Astrocytoma III	25	41	14	11	4	4	11	6
Oligoastrocytoma III	11	39	7	4	—	1	7	3
Oligodendroglioma III	11	49	4	7	2	—	9	—
Glioblastoma WHO IV	19	57	13	6	4	2	8	5
Lymphoma	2	62	1	1	1	1	—	—

stereotactic needle biopsy or open surgical tissue resection. To assess the lesion size, the longest diameter of the contrast-enhancing lesion was measured. In studies without contrast enhancement, the longest diameter of the lesion in the T2-weighted MR image was used.

### Histopathology

Histology was performed for 172 patients either by stereotactic needle biopsy ( $n = 93$ ; 54%) or by open surgical tissue resection ( $n = 79$ ; 46%). The diagnoses were established from formalin-fixed and paraffin-embedded tissue samples as described previously (2).

### Receiver-Operating-Characteristic (ROC) Curve Analysis

The diagnostic accuracy of the  $TBR_{max}$  and  $TBR_{mean}$  of  $^{18}F$ -FET uptake for differentiation of neoplastic lesions from NNLs, for differentiation of HGGs from LGGs, and for differentiation of high-grade tumors (i.e., HGG or lymphoma) from both NNLs and LGGs was evaluated by ROC curve analyses (SigmaPlot, version 11.0; Systat Software Inc.) using subsequent histologic analysis of 172 lesions or clinical course and MR imaging findings ( $n = 2$ ) as a reference. The decision cutoff was considered optimal when the product of paired values for sensitivity and specificity reached its maximum. In addition, the area under the ROC curve (AUC), its SE, and the level of significance were determined as a measure of the diagnostic quality of the test.

### Statistical Analysis

Descriptive statistics are provided as mean and SD or median and range. To compare 2 groups, the Student  $t$  test was used. The Mann-Whitney rank sum test was used when variables were not normally distributed. Probability values of less than 0.05 were considered significant. Statistical analysis was performed using SigmaPlot software (version 11.0; Systat Software Inc.).

## RESULTS

Based on neuropathologic and clinical assessment, we identified 25 patients with NNLs and 145 patients with neoplastic lesions (i.e., LGGs, HGGs, and lymphomas). The results of  $^{18}F$ -FET PET (tumor-to-brain ratios) are summarized in Tables 1 and 2. Further details of each individual patient are given in Supplemental Table 1. The distribution of the  $TBR_{max}$  of  $^{18}F$ -FET uptake in NNLs and gliomas of World Health Organization (WHO) grades I–IV is shown in Figure 1. The corresponding data for the  $TBR_{mean}$  are shown in Figure 2. The data for the 2 lymphomas are not included in the figures. The  $TBR_{max}$  of the 2 lymphomas was 1.9 and 2.9, and the  $TBR_{mean}$  was 1.6 and 2.0 (Supplemental Table 1). For ROC analysis, gliomas of WHO grades III and IV were considered together as HGGs. The 4 lesions classified as occult glioma were not included in the statistical evaluation.

### Differentiation of Neoplastic Lesions from NNLs

Neoplastic lesions showed significantly higher  $^{18}F$ -FET uptake than did NNLs ( $TBR_{max}$ ,  $3.0 \pm 1.3$  vs.  $1.8 \pm 0.5$ ;  $P < 0.001$ ). ROC analysis yielded an optimal cutoff of 2.5 for  $TBR_{max}$  to differentiate between neoplastic lesions and NNLs (sensitivity, 57%; specificity, 92%; accuracy, 62%; area under the curve [AUC], 0.76; 95% confidence interval [CI], 0.68–0.84). The positive predictive value (PPV) was 98%, and the NPV was 27% (Fig. 3). Thus, a  $TBR_{max}$  of more than 2.5 is highly indicative of a neoplastic lesion and suggests that histopathologic confirmation is necessary for further treatment planning.

Similar diagnostic performance was achieved when  $TBR_{mean}$  was used as a parameter (Fig. 3). Neoplastic

**TABLE 2**  
Imaging Results (MR Imaging and  $^{18}\text{F}$ -FET PET)

Diagnosis	MR imaging		$^{18}\text{F}$ -FET-PET TBR			
	Contrast enhancement (n)	Lesion Mean $\pm$ SD (cm)	TBR <sub>max</sub>		TBR <sub>mean</sub>	
			Mean $\pm$ SD	Range	Mean $\pm$ SD	Range
All (n = 174)	76 (44%)	4.3 $\pm$ 2.1	2.8 $\pm$ 1.3	1.0–7.5	1.8 $\pm$ 0.6	0.5–3.5
NNLs (n = 25)	9 (36%)	3.3 $\pm$ 1.7	1.9 $\pm$ 0.5	1.0–2.5	1.4 $\pm$ 0.4	0.5–2.0
Hematoma (n = 4)	3	5.0 $\pm$ 1.8	1.9 $\pm$ 0.4	1.1–2.0	1.5 $\pm$ 0.4	1.1–1.9
Demyelinating lesion (n = 5)	2	2.9 $\pm$ 0.8	2.2 $\pm$ 0.8	1.0–2.3	1.6 $\pm$ 0.5	0.7–2.0
Abscess (n = 6)	2	3.5 $\pm$ 0.9	2.0 $\pm$ 0.5	1.3–2.6	1.5 $\pm$ 0.3	1.2–1.8
Unspecific histology (n = 10)	2	2.7 $\pm$ 2.1	1.6 $\pm$ 0.3	1.2–2.1	1.2 $\pm$ 0.4	0.5–1.7
Neoplastic lesions (n = 149)	67 (45%)	2.9 $\pm$ 1.5	2.9 $\pm$ 1.3	1.0–7.5	1.9 $\pm$ 0.6	0.7–3.8
Occult glioma (n = 4)	1	2.6 $\pm$ 1.0	1.8 $\pm$ 0.7	1.5–2.4	1.4 $\pm$ 0.5	0.7–1.8
Glioma WHO I (n = 4)	2	2.4 $\pm$ 2.7	2.8 $\pm$ 1.9	1.0–3.8	1.7 $\pm$ 0.9	0.7–2.6
Diffuse glioma WHO II (n = 73)	18 (25%)	4.5 $\pm$ 1.7	2.4 $\pm$ 1.0	1.0–5.2	1.6 $\pm$ 0.5	0.7–2.8
Astrocytoma II (n = 53)	13	4.8 $\pm$ 1.7	2.3 $\pm$ 0.9	1.0–5.1	1.6 $\pm$ 0.5	0.7–2.8
Oligoastrocytoma II (n = 12)	3	4.3 $\pm$ 1.5	2.7 $\pm$ 1.1	1.8–5.2	1.8 $\pm$ 0.4	1.1–2.6
Oligodendroglioma II (n = 6)	0	3.6 $\pm$ 1.3	2.6 $\pm$ 1.1	1.1–3.0	1.7 $\pm$ 0.5	0.9–2.2
Ependymoma II (n = 2)	2	1.5 $\pm$ 1.0	2.7 $\pm$ 1.1	1.9–3.5	1.9 $\pm$ 0.4	1.6–2.2
Anaplastic glioma WHO III (n = 47)	27 (57%)	4.9 $\pm$ 2.5	3.5 $\pm$ 1.5	1.2–6.9	2.1 $\pm$ 0.7	0.7–3.8
Astrocytoma III (n = 25)	11	4.7 $\pm$ 2.5	3.3 $\pm$ 1.5	1.2–6.3	2.0 $\pm$ 0.7	0.7–3.8
Oligoastrocytoma III (n = 11)	8	6.0 $\pm$ 3.0	3.5 $\pm$ 1.4	1.3–5.4	2.0 $\pm$ 0.6	0.9–2.6
Oligodendroglioma III (n = 11)	8	4.3 $\pm$ 1.5	4.0 $\pm$ 1.4	2.2–6.9	2.3 $\pm$ 0.5	1.7–3.0
Glioblastoma WHO IV (n = 19)	18 (95%)	3.7 $\pm$ 1.6	3.9 $\pm$ 1.2	2.6–7.5	2.3 $\pm$ 0.3	1.9–3.2
Lymphoma (n = 2)	1	6.7 $\pm$ 7.3	2.4 $\pm$ 0.7	1.9–2.9	1.8 $\pm$ 0.3	1.6–2.0

lesions showed significantly higher TBR<sub>mean</sub> than did NNLs (TBR<sub>mean</sub>, 1.9  $\pm$  0.6 vs. 1.4  $\pm$  0.4;  $P < 0.001$ ). ROC analysis yielded an optimal cutoff of 1.9 for TBR<sub>mean</sub> to differentiate between neoplastic lesions and NNLs (sensitivity, 58%; specificity, 88%; accuracy, 62%; AUC, 0.74; 95% CI, 0.66–0.82). The PPV was 97%, and the NPV was 27%.

#### Differentiation of HGG from LGG

Patients with HGGs ( $n = 66$ ) exhibited significantly higher  $^{18}\text{F}$ -FET uptake than did patients with LGGs ( $n = 77$ ) (TBR<sub>max</sub>, 3.6  $\pm$  1.4 vs. 2.4  $\pm$  1.0;  $P < 0.001$ ). ROC analysis for differentiation between HGG and LGG yielded an optimal cutoff of 2.5 for TBR<sub>max</sub> (sensitivity, 80%; specificity, 65%; accuracy, 72%; AUC, 0.77; 95% CI, 0.68–0.84) (ROC curve not shown). The PPV was 66%, and the NPV was 79%. These values were not sufficient to justify a clinical decision, and a biopsy to determine the therapeutic procedure could not be avoided.

Similar diagnostic performance was achieved when TBR<sub>mean</sub> was used as a parameter. HGGs showed a significantly higher TBR<sub>mean</sub> than did LGGs (TBR<sub>mean</sub>, 2.1  $\pm$  0.6 vs. 1.6  $\pm$  0.5;  $P < 0.001$ ). ROC analysis yielded an optimal cutoff of 1.9 for TBR<sub>mean</sub> to differentiate between HGGs and LGGs (sensitivity, 82%; specificity, 62%; accuracy, 71%; AUC, 0.74; 95% CI, 0.67–0.83). The PPV was 65%, and the NPV was 80%.

#### Differentiation of High-Grade Tumors from NNLs and LGGs

The best differentiation between high-grade tumors (i.e., HGG and lymphoma) and both NNLs and LGGs (TBR<sub>max</sub>,

3.6  $\pm$  1.4 vs. 2.3  $\pm$  0.9;  $P < 0.001$ ) was achieved with a cutoff of 2.5 for TBR<sub>max</sub> (sensitivity, 79%; specificity, 72%; accuracy, 75%; AUC, 0.79; 95% CI, 0.71–0.86) (Fig. 4). The PPV was 65%, and the NPV was 84%. Thus, a TBR<sub>max</sub> of less than 2.5 suggests that a high-grade tumor is unlikely.

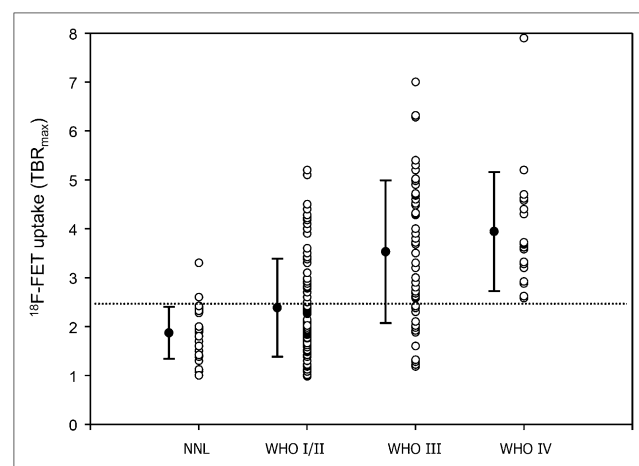


**FIGURE 1.** Distribution of TBR<sub>max</sub> of  $^{18}\text{F}$ -FET uptake in NNL and gliomas of WHO grades I/II, III, and IV. Dotted line indicates optimal cutoff of 2.5 determined by ROC analysis to differentiate between neoplastic lesions and NNL. This cutoff also differentiates best between LGG (WHO grades I and II) and HGG (WHO grades III and IV), as well as between high-grade tumors (HGG and lymphomas) and NNL or LGG.

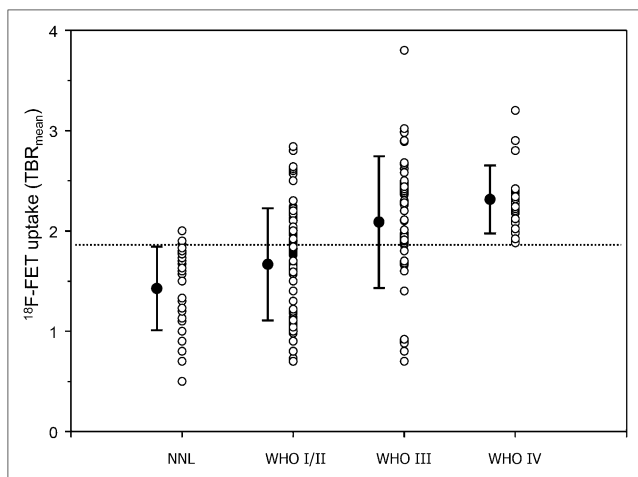


**FIGURE 2.** Distribution of  $TBR_{mean}$  of  $^{18}F$ -FET uptake in NNL and gliomas of WHO grades I/II, III, and IV. Dotted line indicates optimal cutoff of 1.9 determined by ROC analysis to differentiate between neoplastic lesions and NNL. This cutoff also differentiates best between LGG (WHO grades I and II) and HGG (WHO grades III and IV), as well as between high-grade tumors (HGG and lymphomas) and NNL or LGG.

A similar diagnostic performance was achieved when  $TBR_{mean}$  was used as a parameter. HGGs and lymphomas showed a significantly higher  $TBR_{mean}$  than did NNLs and LGGs ( $TBR_{mean}$ ,  $2.1 \pm 0.6$  vs.  $1.6 \pm 0.5$ ;  $P < 0.001$ ). ROC analysis yielded an optimal cutoff of 1.9 for  $TBR_{mean}$  to differentiate between tumors and NNLs (sensitivity, 81%; specificity, 69%; accuracy, 74%; AUC, 0.78; 95% CI, 0.70–0.85) (Fig. 4). The PPV was 63%, and the NPV was 84%.

## DISCUSSION

This study on a relatively large group of selected patients with untreated primary brain tumors and histopathologic confirmation demonstrated that there is wide variability in  $^{18}F$ -FET uptake ratios for cerebral gliomas of different WHO grades and TBRs of  $^{18}F$ -FET uptake. These observations are in line with those of several other studies (2,10,13,14). Nevertheless, we identified threshold values for  $TBR_{max}$  and  $TBR_{mean}$  that may be helpful in the clinical decision-making process. For neoplastic lesions,  $^{18}F$ -FET uptake beyond a  $TBR_{max}$  cutoff of 2.5 or a  $TBR_{mean}$  cutoff of 1.9 had a PPV of 98% or 97%, respectively. Furthermore, for high-grade tumors such as HGGs or lymphomas,  $^{18}F$ -FET uptake with a  $TBR_{max}$  of less than 2.5 or a  $TBR_{mean}$  of less than 1.9 had an NPV of 84%.

This information might be helpful for the neurooncologist who is deciding on patient management. If a benign lesion can be excluded by  $^{18}F$ -FET PET with high probability, the need for an immediate histologic examination is a given. On the other hand, when the clinical course and MR imaging suggest a benign process, the finding of low  $^{18}F$ -FET uptake may support a decision to observe the process temporarily.

The selection of patients in this study was based on the challenge to improve diagnostic information about cerebral

lesions suspected of being a glioma on the basis of MR imaging results and for which either the extent and optimal biopsy site or differentiation from an NNL is unclear. As this challenge concerns in particular tumors that exhibit no contrast enhancement on MR imaging, the patient population included more patients with WHO grade II and III gliomas than are normally found. However, there is no consequent restriction on the validity of our study since  $^{18}F$ -FET PET is particularly required by the neurooncologist in these patients.

The results of our study are similar to those of previous studies. In a study evaluating  $^{11}C$ -MET PET in a consecutive series of 196 patients with suspected brain tumors, gliomas could be differentiated from NNLs with a sensitivity of 76% and a specificity of 87% using a threshold of 1.47 for  $TBR_{mean}$ . From these values, a  $TBR_{mean}$  greater than 1.47 has a positive likelihood ratio of 5.85 for a tumor, compared with 4.83 using a  $TBR_{mean}$  greater than 1.9 in our study. The negative likelihood ratio for a tumor at a  $TBR_{mean}$  of less than 1.47 in that study was 0.28, compared with 0.48 in our study. That is, the NPV of low amino acid uptake to exclude a tumor is limited, because approximately 30% of LGGs exhibit low or absent amino acid uptake (14,15). The difference between the threshold in the above-mentioned study and that in our study may be explained by differences in the definition of the tumor ROI, since the  $TBR_{mean}$  is dependent on the size of the tumor ROI.

Another study focused on the role of  $^{18}F$ -FET PET in the initial evaluation of 88 patients with brain lesions (10).

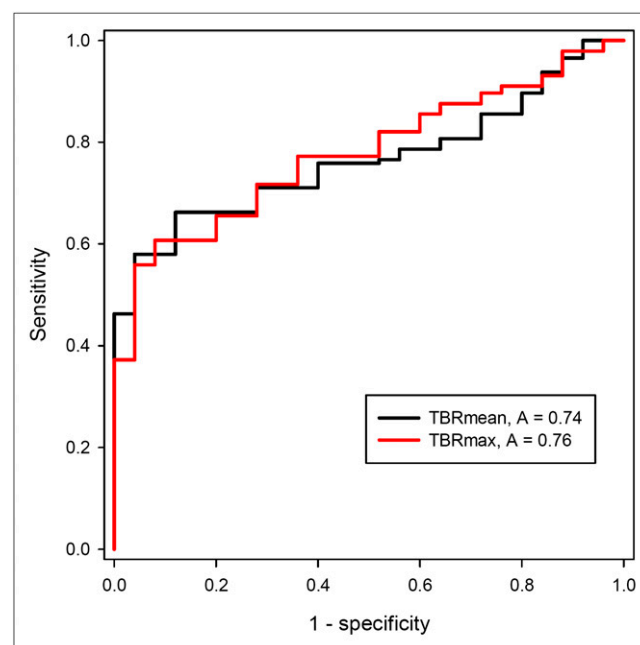


**FIGURE 3.** ROC curve analysis of  $TBR_{mean}$  (black curve) and  $TBR_{max}$  (red curve) to differentiate between neoplastic lesions and NNL. Area under curve was 0.74 for  $TBR_{mean}$  ( $P < 0.001$ ; 95% CI, 0.66–0.82; optimal cutoff, 1.9) and 0.76 for  $TBR_{max}$  ( $P < 0.001$ ; 95% CI, 0.68–0.84; optimal cutoff, 2.5).

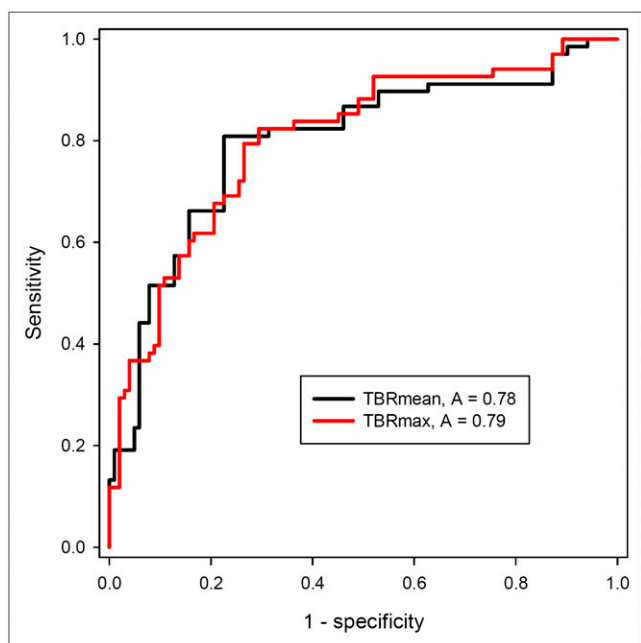


**FIGURE 4.** ROC curve analysis of  $TBR_{mean}$  (red curve) and  $TBR_{max}$  (black curve) to differentiate between high-grade tumors (i.e., HGG and lymphoma) and LGG/NNL. Area under curve was 0.78 for  $TBR_{mean}$  ( $P < 0.001$ ; 95% CI, 0.70–0.85; optimal cutoff, 1.9) and 0.79 for  $TBR_{max}$  ( $P < 0.001$ ; 95% CI, 0.72–0.86; optimal cutoff, 2.5).

However, in that study images were interpreted visually and the diagnostic accuracy cannot be compared properly to that in our study. The sensitivity for detecting a malignant tumor was 93%, compared with 81% in our study, and the NPV for a malignant entity was 89%, compared with 86% in our study. Thus, the results are similar despite methodology differences.

Recently, a metaanalysis evaluated the performance of  $^{18}F$ -FET PET in the differential diagnosis of 401 patients with primary brain tumors (11). A limitation of that particular metaanalysis is the fact that the methods for the ROI definition and acquisition times varied among the different studies. Moreover, 7 of the 13 studies that focused on various clinical topics came from one center (2,15–20) and 2 from another center (21,22). In the patient populations of those studies, there appears to be an overlap that was not considered in the metaanalysis.

In that study, ROC analysis yielded an optimal threshold of 1.6 for  $TBR_{mean}$  and 2.1 for  $TBR_{max}$  to differentiate primary brain tumors from NNLS—thresholds that are somewhat lower than that observed in our study. With respect to the different methodologies of the studies, the authors emphasized that those thresholds should be considered with caution and that further investigations with strict standardization of PET acquisition protocols are necessary. We would like to emphasize that our study meets these criteria.

Great importance was placed on the objectivity and reproducibility of the methodology. The tumor borders were defined by a lesion-to-brain ratio greater than 1.6,

which is based on a previous biopsy-controlled study (2). Furthermore, the evaluation of  $TBR_{max}$  and  $TBR_{mean}$  yielded similar diagnostic accuracy concerning the differentiation of brain lesions, but both parameters have limitations that need to be considered. Although mean  $TBR_{mean}$  is influenced by the size of the tumor ROI,  $TBR_{max}$  is dependent on the spatial resolution of the PET scanner and on the reconstruction matrix. Therefore, it is important to adapt the evaluation methods such that the data among various centers are comparable. In addition, the timing of data acquisition plays an important role since the TBR varies over time depending on the grade of malignancy. Therefore, in our study all data that were acquired during the last 10 y were reconstructed again using the summarized data from 20 to 40 min to determine the TBR.

The metaanalysis mentioned above (11) yielded a pooled sensitivity of 82% for primary brain tumors and a specificity of 76%, and the authors emphasized the excellent performance of  $^{18}F$ -FET PET for diagnosing primary brain tumors. Although we cannot accept this view entirely, we agree that important information may be extracted from  $^{18}F$ -FET PET during the initial diagnosis. The diagnostic value of  $^{18}F$ -FET PET during the initial diagnosis of cerebral lesions lies especially in defining an optimal site for biopsy and determining the extent of metabolically active tumor for treatment planning rather than in making a differential diagnosis of the lesion. A recent analysis indicated the cost-effectiveness of  $^{18}F$ -FET PET-guided biopsy (23).

With respect to differentiation between HGGs and LGGs, it is evident that there is a wide overlap of uptake ratios between gliomas of different WHO grades. The diagnostic accuracy of  $^{18}F$ -FET PET is not sufficient to decisively influence the therapeutic approach, and histopathologic confirmation by biopsy or open surgery remains necessary.

Several studies have indicated that the evaluation of  $^{18}F$ -FET kinetics may allow differentiation between HGGs and LGGs with higher sensitivity and specificity (13,14,24–27). HGGs appear to be characterized by an early peak around 10–15 min after injection followed by a decrease in  $^{18}F$ -FET uptake. In contrast, steadily increasing time-activity curves seem to be typical for LGGs. Unfortunately, such data were not available for most of the patients included in this study.

## CONCLUSION

$^{18}F$ -FET uptake ratios provide valuable additional information for the differentiation of cerebral lesions and the grading of gliomas.  $^{18}F$ -FET uptake with a  $TBR_{max}$  of more than 2.5 has a high PPV for a neoplastic lesion, and a  $TBR_{max}$  of less than 2.5 has a high NPV for a high-grade tumor (i.e., HGG or lymphoma), which may be helpful for the neurooncologist in the clinical decision-making process. Thus,  $^{18}F$ -FET PET may add relevant complementary information to clinical data and MR imaging in the clinical setting.

## DISCLOSURE

The costs of publication of this article were defrayed in part by the payment of page charges. Therefore, and solely to indicate this fact, this article is hereby marked “advertisement” in accordance with 18 USC section 1734. The Brain Imaging Center West (BICW) supported this work. No other potential conflict of interest relevant to this article was reported.

## ACKNOWLEDGMENTS

We thank Suzanne Schaden, Elisabeth Theelen, and Kornelia Frey for assistance with the patient studies and Johannes Ermer, Silke Grafmüller, Erika Wabbals, and Sascha Rehbein for radiosynthesis of  $^{18}\text{F}$ -FET.

## REFERENCES

1. Cha S. Neuroimaging in neuro-oncology. *Neurotherapeutics*. 2009;6:465–477.
2. Pauleit D, Floeth F, Hamacher K, et al. O-(2-[ $^{18}\text{F}$ ]fluoroethyl)-L-tyrosine PET combined with MRI improves the diagnostic assessment of cerebral gliomas. *Brain*. 2005;128:678–687.
3. Galldiks N, Langen K, Holy R, et al. Assessment of treatment response in patients with glioblastoma using [ $^{18}\text{F}$ ]fluoroethyl-L-tyrosine PET in comparison to MRI. *J Nucl Med*. 2012;53:1048–1057.
4. Pöppel G, Götz C, Rachinger W, Gildehaus FJ, Tonn JC, Tatsch K. Value of O-(2-[ $^{18}\text{F}$ ]fluoroethyl)-L-tyrosine PET for the diagnosis of recurrent glioma. *Eur J Nucl Med Mol Imaging*. 2004;31:1464–1470.
5. Singhal T, Narayanan TK, Jain V, Mukherjee J, Mantil J.  $^{11}\text{C}$ -L-methionine positron emission tomography in the clinical management of cerebral gliomas. *Mol Imaging Biol*. 2008;10:1–18.
6. Langen KJ, Hamacher K, Weckesser M, et al. O-(2-[ $^{18}\text{F}$ ]fluoroethyl)-L-tyrosine: uptake mechanisms and clinical applications. *Nucl Med Biol*. 2006;33:287–294.
7. Wester HJ, Herz M, Weber W, et al. Synthesis and radiopharmacology of O-(2-[ $^{18}\text{F}$ ]fluoroethyl)-L-tyrosine for tumor imaging. *J Nucl Med*. 1999;40:205–212.
8. Grosu AL, Astner ST, Riedel E, et al. An interindividual comparison of O-(2-[ $^{18}\text{F}$ ]fluoroethyl)-L-tyrosine (FET)- and L-[methyl- $^{11}\text{C}$ ]methionine (MET)-PET in patients with brain gliomas and metastases. *Int J Radiat Oncol Biol Phys*. 2011;81:1049–1058.
9. Herholz K, Holzer T, Bauer B, et al.  $^{11}\text{C}$ -methionine PET for differential diagnosis of low-grade gliomas. *Neurology*. 1998;50:1316–1322.
10. Pichler R, Dunzinger A, Wurm G, et al. Is there a place for FET PET in the initial evaluation of brain lesions with unknown significance? *Eur J Nucl Med Mol Imaging*. 2010;37:1521–1528.
11. Dunet V, Rossier C, Buck A, Stupp R, Prior JO. Performance of  $^{18}\text{F}$ -fluoro-ethyl-tyrosine ( $^{18}\text{F}$ -FET) PET for the differential diagnosis of primary brain tumor: a systematic review and metaanalysis. *J Nucl Med*. 2012;53:207–214.
12. Hamacher K, Coenen HH. Efficient routine production of the  $^{18}\text{F}$ -labelled amino acid O-2- $^{18}\text{F}$  fluoroethyl-L-tyrosine. *Appl Radiat Isot*. 2002;57:853–856.
13. Pöppel G, Kreth FW, Mehrkens JH, et al. FET PET for the evaluation of untreated gliomas: correlation of FET uptake and uptake kinetics with tumour grading. *Eur J Nucl Med Mol Imaging*. 2007;34:1933–1942.
14. Jansen NL, Graute V, Armbruster L, et al. MRI-suspected low-grade glioma: is there a need to perform dynamic FET PET? *Eur J Nucl Med Mol Imaging*. 2012;39:1021–1029.
15. Floeth FW, Pauleit D, Sabel M, et al. Prognostic value of O-(2- $^{18}\text{F}$ -fluoroethyl)-L-tyrosine PET and MRI in low-grade glioma. *J Nucl Med*. 2007;48:519–527.
16. Pauleit D, Stoffels G, Bachofner A, et al. Comparison of  $^{18}\text{F}$ -FET and  $^{18}\text{F}$ -FDG PET in brain tumors. *Nucl Med Biol*. 2009;36:779–787.
17. Pauleit D, Floeth F, Tellmann L, et al. Comparison of O-(2- $^{18}\text{F}$ -fluoroethyl)-L-tyrosine PET and 3- $^{123}\text{I}$ -iodo-alpha-methyl-L-tyrosine SPECT in brain tumors. *J Nucl Med*. 2004;45:374–381.
18. Floeth FW, Pauleit D, Sabel M, et al.  $^{18}\text{F}$ -FET PET differentiation of ring-enhancing brain lesions. *J Nucl Med*. 2006;47:776–782.
19. Floeth FW, Pauleit D, Wittsack HJ, et al. Multimodal metabolic imaging of cerebral gliomas: positron emission tomography with [ $^{18}\text{F}$ ]fluoroethyl-L-tyrosine and magnetic resonance spectroscopy. *J Neurosurg*. 2005;102:318–327.
20. Floeth FW, Sabel M, Ewelt C, et al. Comparison of  $^{18}\text{F}$ -FET PET and 5-ALA fluorescence in cerebral gliomas. *Eur J Nucl Med Mol Imaging*. 2011;38:731–741.
21. Plotkin M, Blechschmidt C, Auf G, et al. Comparison of F-18 FET-PET with F-18 FDG-PET for biopsy planning of non-contrast-enhancing gliomas. *Eur Radiol*. 2010;20:2496–2502.
22. Stockhammer F, Plotkin M, Amthauer H, van Landeghem FK, Woiciechowsky C. Correlation of F-18-fluoro-ethyl-tyrosine uptake with vascular and cell density in non-contrast-enhancing gliomas. *J Neurooncol*. 2008;88:205–210.
23. Heinzel A, Stock S, Langen KJ, Müller D. Cost-effectiveness analysis of FET PET-guided target selection for the diagnosis of gliomas. *Eur J Nucl Med Mol Imaging*. 2012;39:1089–1096.
24. Weckesser M, Langen KJ, Rickert CH, et al. O-(2-[ $^{18}\text{F}$ ]fluoroethyl)-L-tyrosine PET in the clinical evaluation of primary brain tumours. *Eur J Nucl Med Mol Imaging*. 2005;32:422–429.
25. Calcagni ML, Galli G, Giordano A, et al. Dynamic O-(2-[ $^{18}\text{F}$ ]fluoroethyl)-L-tyrosine (F-18 FET) PET for glioma grading: assessment of individual probability of malignancy. *Clin Nucl Med*. 2011;36:841–847.
26. Kunz M, Thon N, Eigenbrod S, et al. Hot spots in dynamic  $^{18}\text{F}$ -FET-PET delineate malignant tumor parts within suspected WHO grade II gliomas. *Neuro-oncol*. 2011;13:307–316.
27. Pöppel G, Kreth FW, Herms J, et al. Analysis of  $^{18}\text{F}$ -FET PET for grading of recurrent gliomas: is evaluation of uptake kinetics superior to standard methods? *J Nucl Med*. 2006;47:393–403.